Supplementary Information

The Evolution of Turbulent Micro-vortices and their Effect on Convection Heat Transfer in Porous Media

Ching-Wei Huang, Vishal Srikanth, Andrey V. Kuznetsov

Supplementary figures

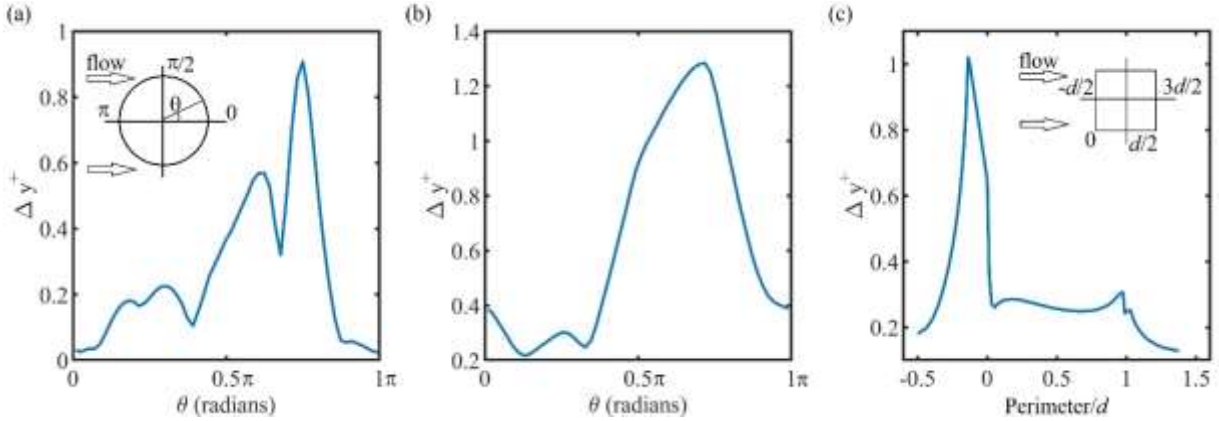

Figure S1: The distribution of the Reynolds average of the non-dimensional wall grid spacing Δy^+ on the surface of the solid obstacle for case (a) A1, (b) A2, and (c) A3. Note that only the distribution on one half of the surface is plotted since the distribution is symmetric.

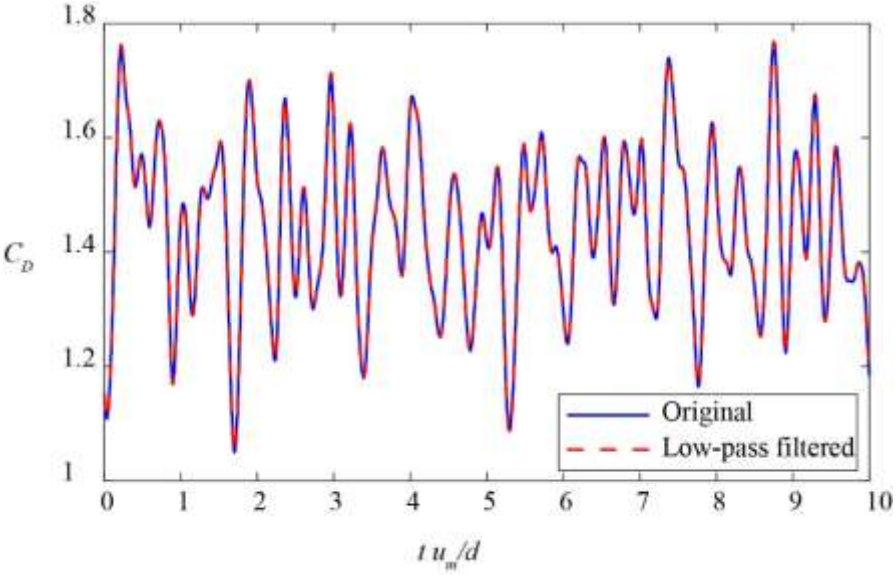

Figure S2: The coefficient of drag on a single solid obstacle for case A1 versus dimensionless time. The results in the figure show that filtering the signal above a frequency of 100 has an insignificant impact on the original signal.

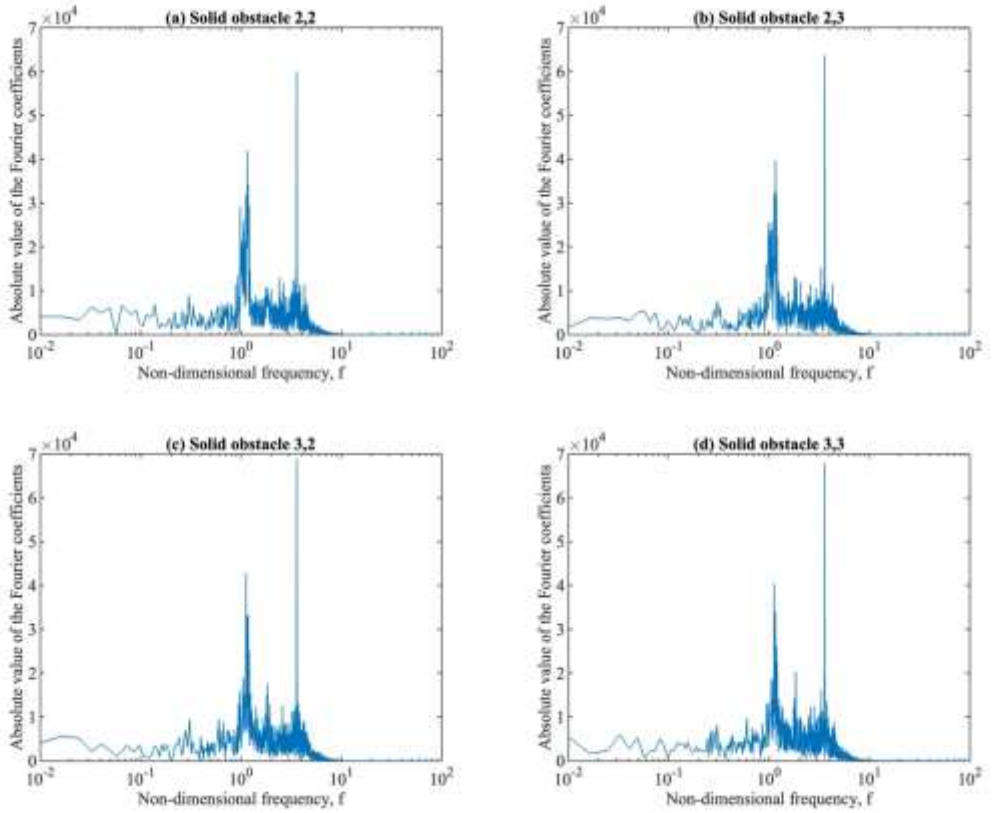

Figure S3: Frequency spectrum of the lift coefficient acting on different solid obstacles inside the REV for case A1. The comparison is shown here to demonstrate that the peaks in the spectra are identical across the different solid obstacles.

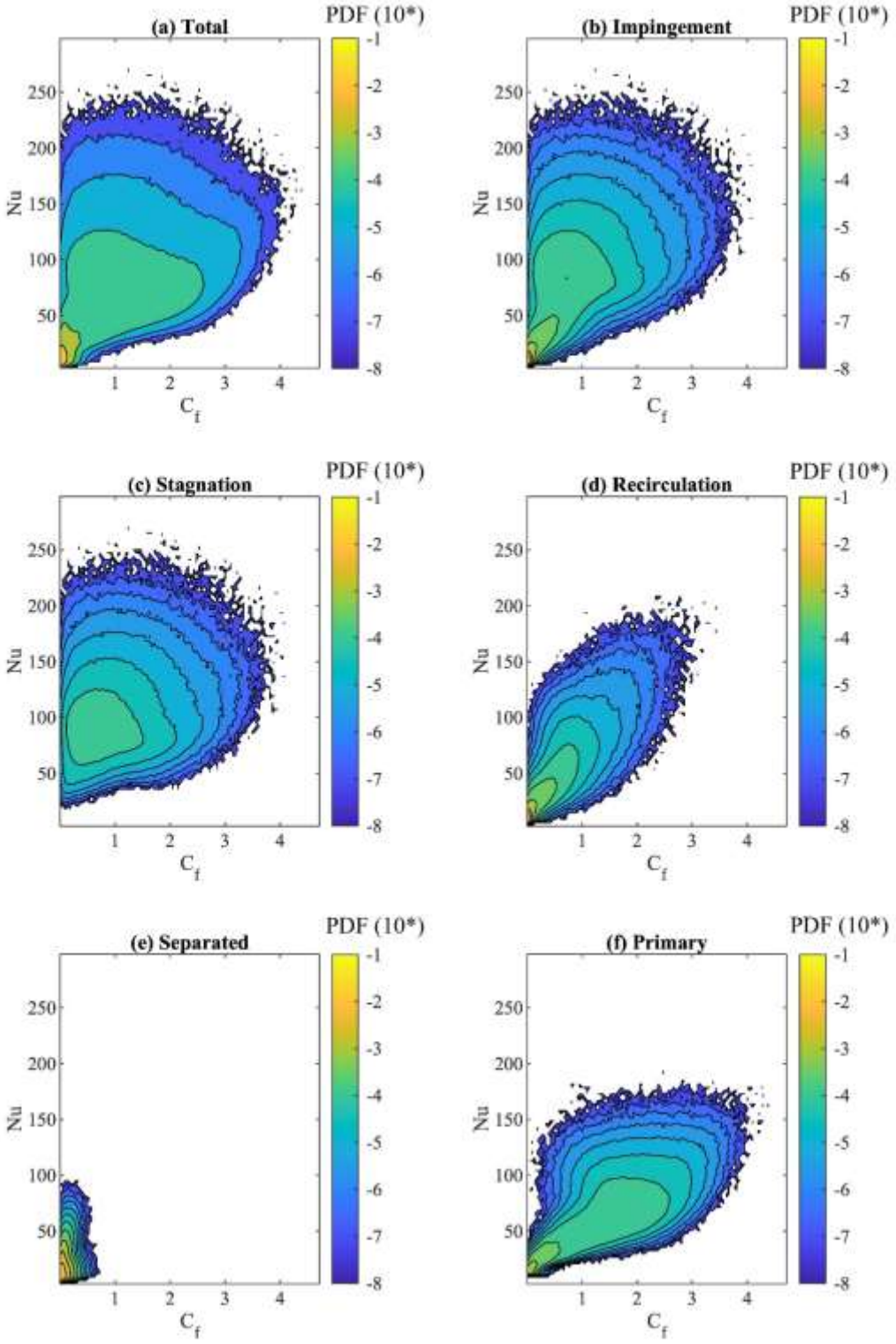

Figure S4: The C_f-Nu probability density function for the different regions on the solid obstacle for case A1. This supplementary figure shows the components of figure 11(a) in the manuscript.

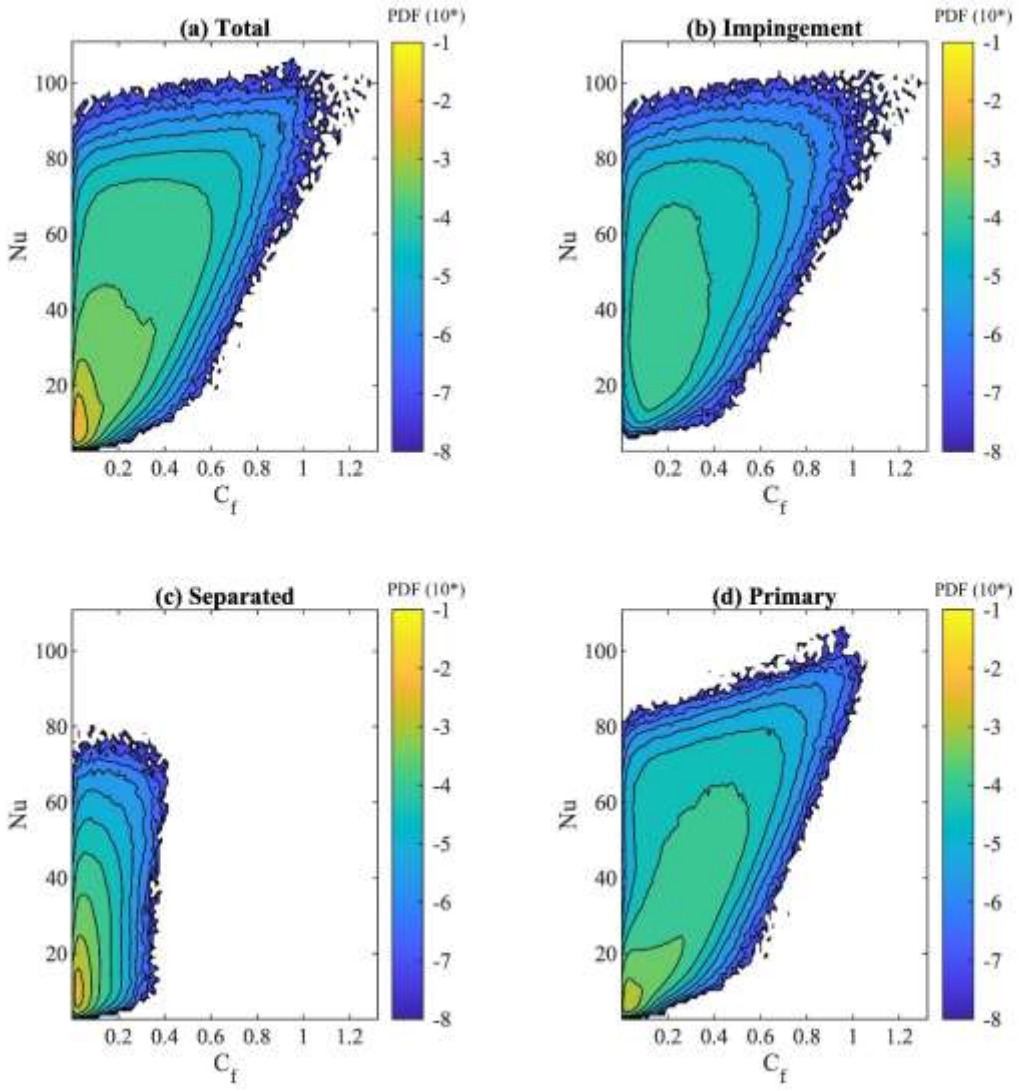

Figure S5: The C_f-Nu probability density function for the different regions on the solid obstacle for case A2. This supplementary figure shows the components of figure 11(b) in the manuscript.

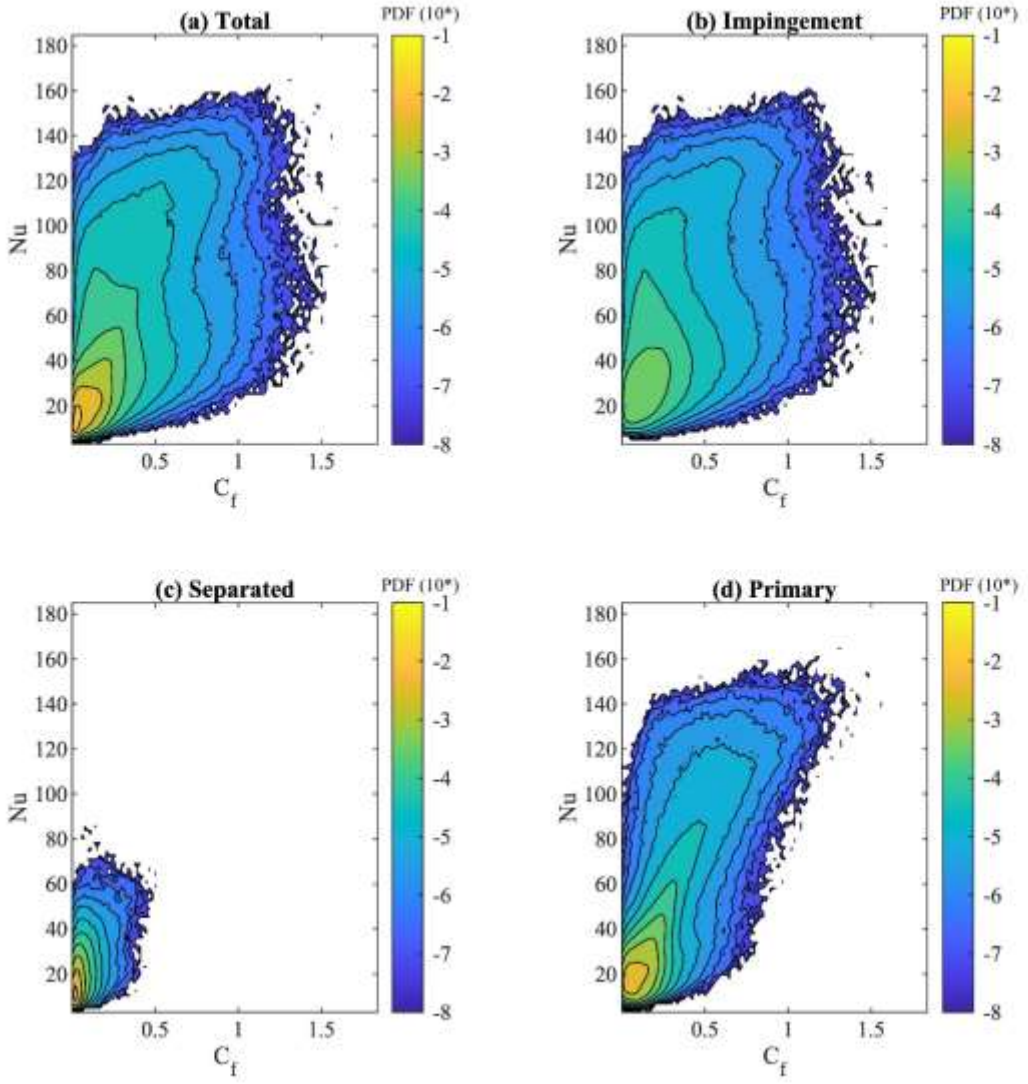

Figure S6: The C_f-Nu probability density function for the different regions on the solid obstacle for case A3. This supplementary figure shows the components of figure 11(c) in the manuscript.

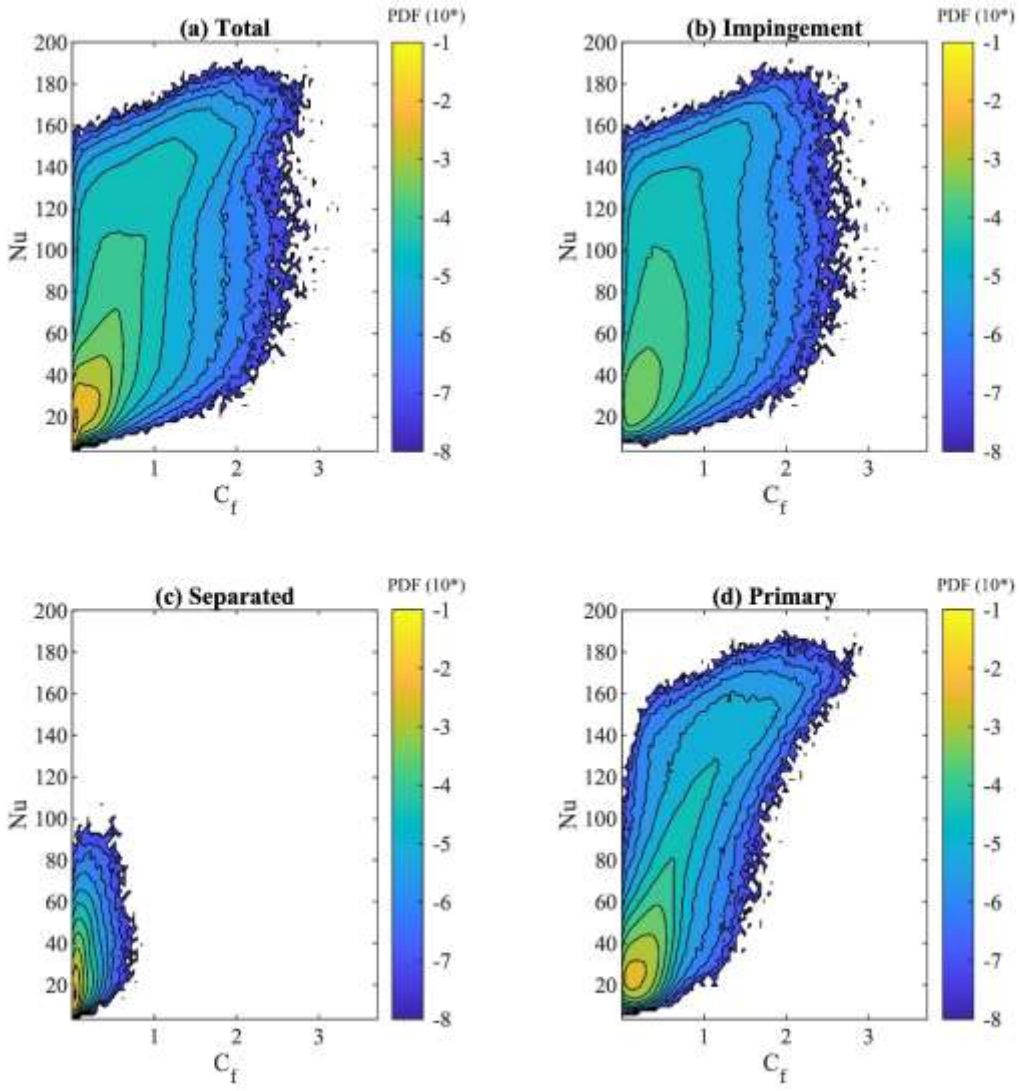

Figure S7: The C_f-Nu probability density function for the different regions on the solid obstacle for case A4. This supplementary figure shows the components of figure 11(d) in the manuscript.

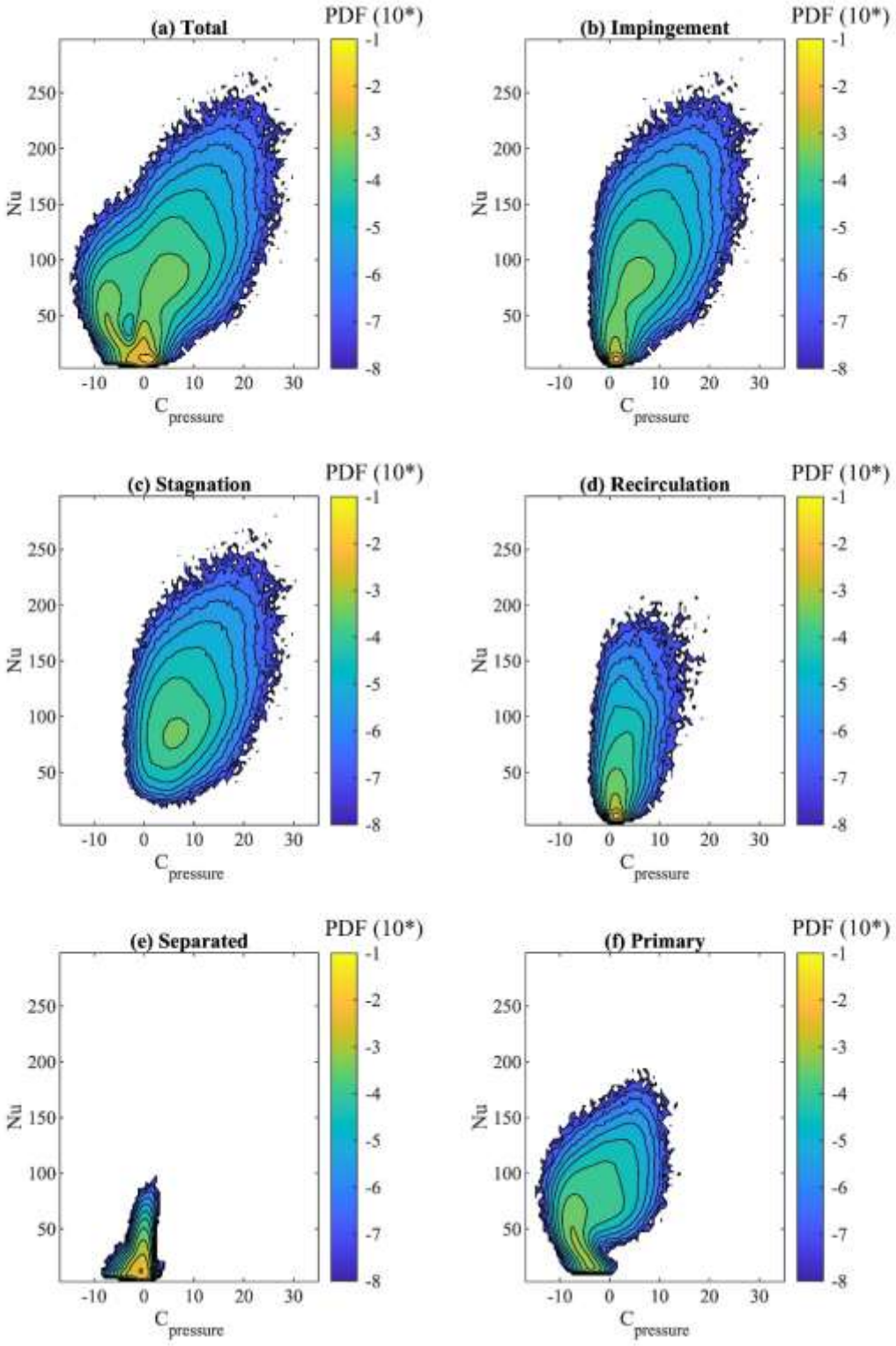

Figure S8: The $C_{pressure}$-Nu probability density function for the different regions on the solid obstacle for case A1. This supplementary figure shows the components of figure 12(a) in the manuscript.

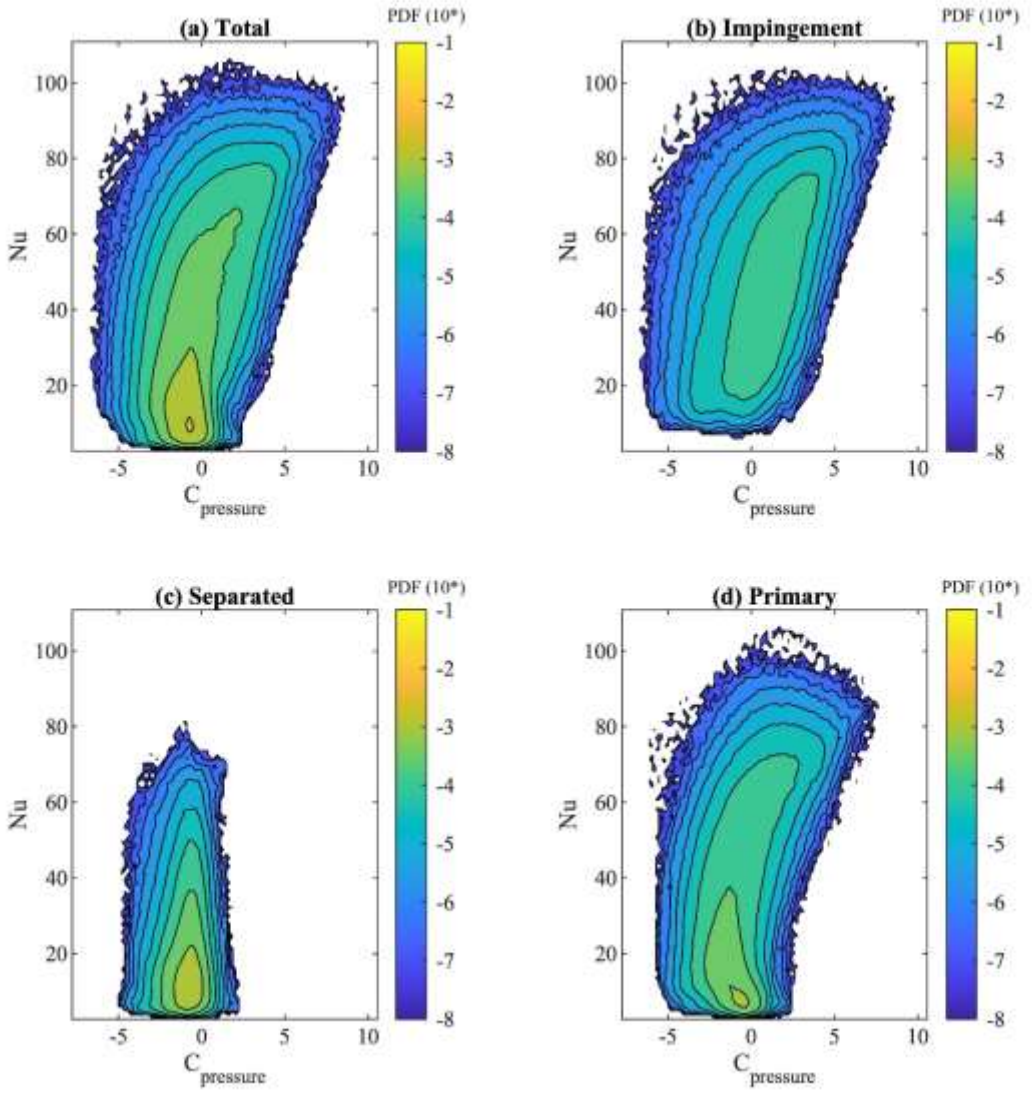

Figure S9: The $C_{pressure}$-Nu probability density function for the different regions on the solid obstacle for case A2. This supplementary figure shows the components of figure 12(b) in the manuscript.

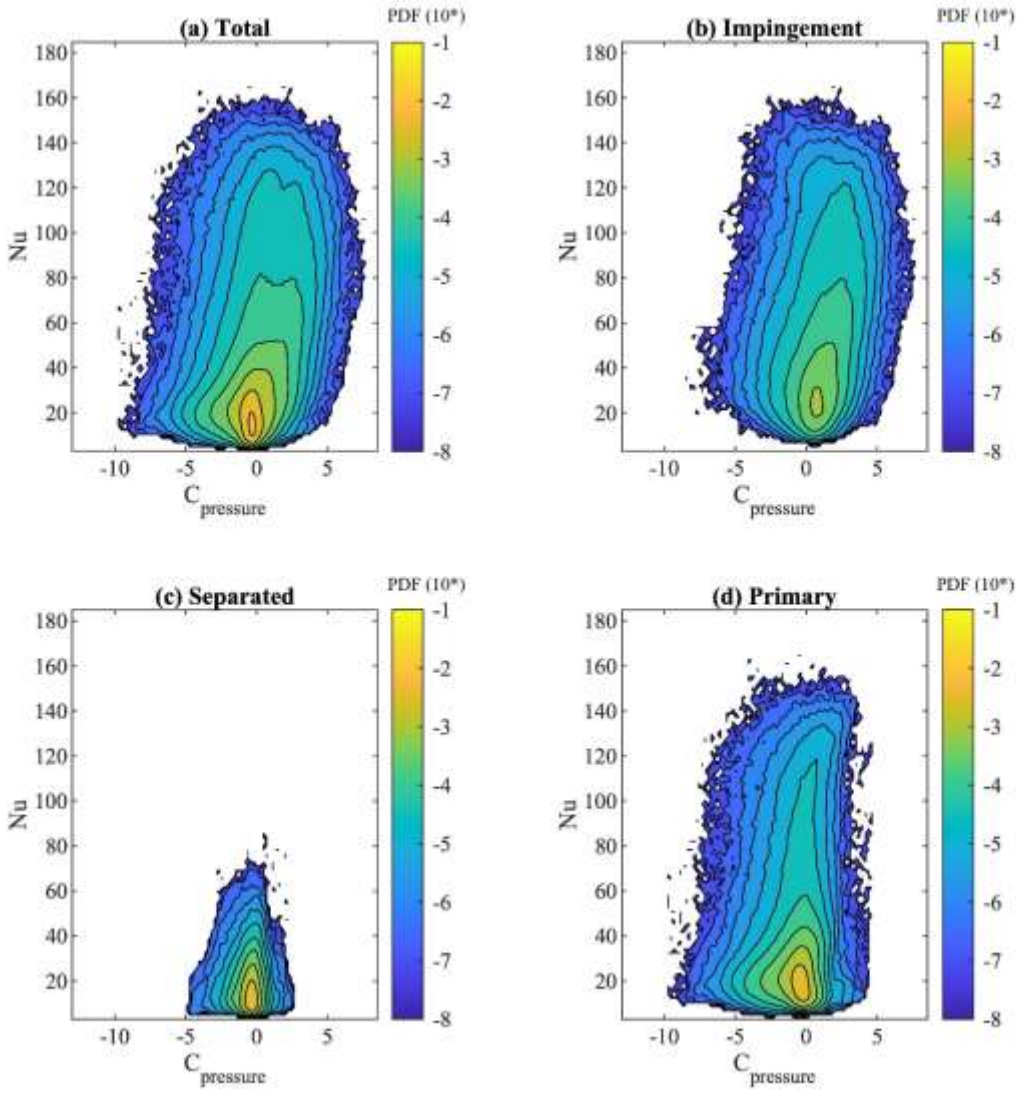

Figure S10: The $C_{pressure}$-Nu probability density function for the different regions on the solid obstacle for case A3. This supplementary figure shows the components of figure 12(c) in the manuscript.

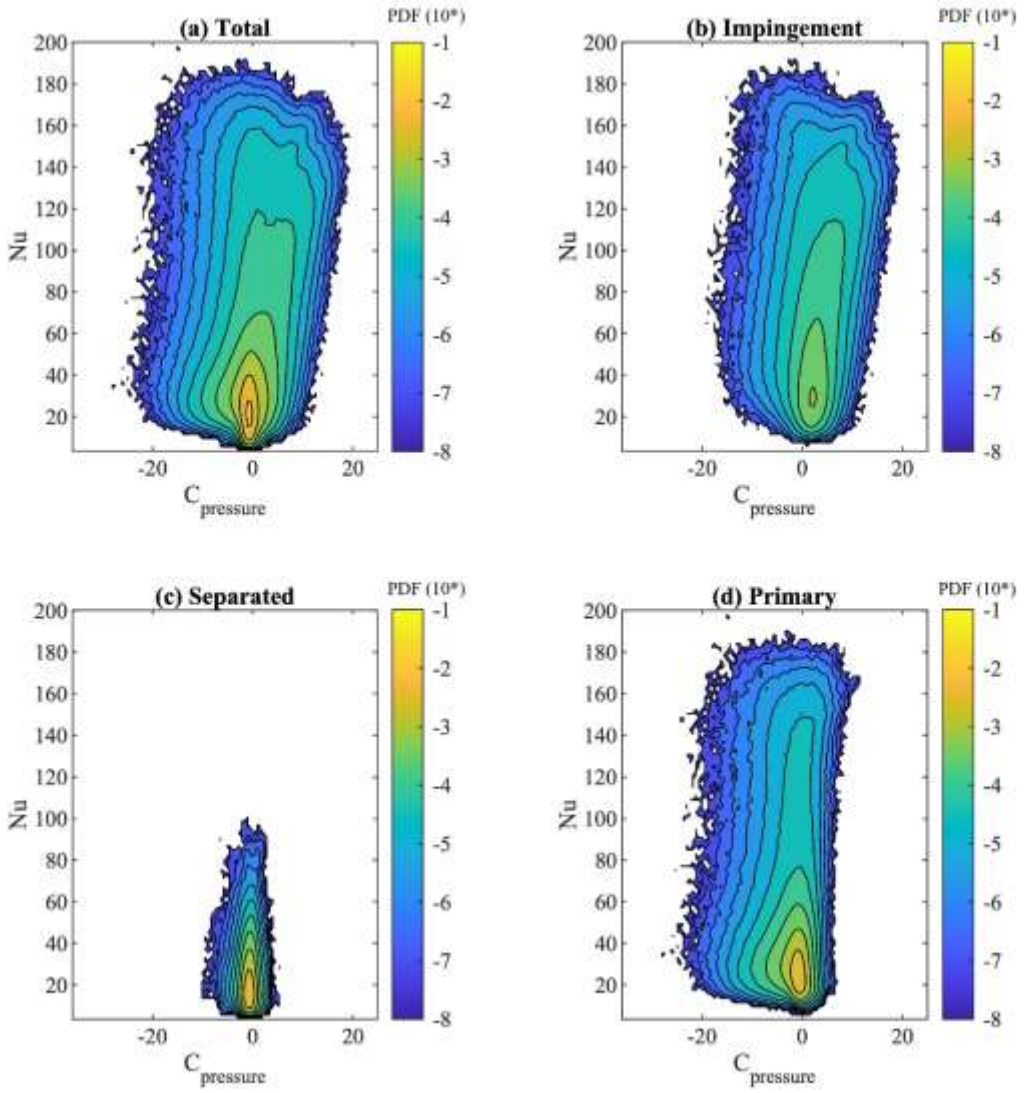

Figure S11: The $C_{pressure}$-Nu probability density function for the different regions on the solid obstacle for case A4. This supplementary figure shows the components of figure 12(d) in the manuscript.